Progress In Electromagnetics Research, PIER 51, 249–279, 2005

EXPERIMENTAL STUDY ON SEVERAL LEFT-HANDED METAMATERIALS

L. Ran, J. Huangfu, H. Chen, X. Zhang, and K. Cheng

Department of Information and Electronic Engineering
Zhejiang University
Hangzhou, China

T. M. Grzegorczyk and J. A. Kong

Department of Electrical Engineering and Computer Science
MIT, Cambridge, MA 02139, USA

Abstract—Left-handed materials (LHM) are engineered structures that exhibit electromagnetic properties not found in nature. Real applications of LHM need substrates with low loss, wide bandwidth as well as stable mechanical characteristics. In this paper, we summarize some experimental as well as numerical results of left-handed materials with different configurations of rods and split-ring resonators (SRRs). Hot-press technics utilized in PC board manufacture are used to produce solid-state multi-layer left-handed materials. Either mechanical or electromagnetic characteristics of LH samples are notably improved.

1. INTRODUCTION

Left-handed metamaterials (LHM) are engineered structures that exhibit electromagnetic properties not found in nature. Early in 1968, V. G. Veselago introduced the concept of left-handed (LH) materials, and described their distinct properties, such as a reversed Doppler effect, a reversed Snell refraction and a reversed Cerenkov radiation [1]. In 2001, D. R. Smith et al. fabricated a metamaterial sample by periodically arranging rods and split-ring resonators (SRR) into an arrays, and for the first time verified the real existence of left-handed material by observing a "negative" refraction of a microwave beam transmitted through a prism-shaped sample [2]. Currently, many possible applications of left-handed materials have been proposed, such as flat lens [3], thin resonators [4], filters and antennas [5]. However,

before these applications could be realized, low loss, wide bandwidth left-handed materials with stable mechanical and electromagnetic characteristics should be produced. This means that more work is needed in the development of various structures or configurations of left-handed materials in order to be able to choose the suitable ones for different applications. In addition, proper manufacturing techniques are also needed for mass production. In this paper, we describe some experimental as well as numerical results of left-handed materials with different configurations of rods and/or split-ring resonators (SRRs) [6]. Hot-press technics utilized in PC board manufacture are used to produce solid-state multi-layer left-handed materials. In this paper, we report a solid-state sample exhibiting insertion losses of about 0.4–0.5 dB per unit cell for a bandwidth up to 2.6 GHz. Such a metamaterial could already be used for real applications.

2. METHODS

In this section, we describe the designing methodologies, the experimental setups and the production technics utilized in our work. The general steps we have adopted for the design of LHM are as follows: first, we choose a structure of SRR, for which we calculate the resonant frequency according to the dimensions and adjust it into X-band, where our measurement capabilities are. Then we perform simulations and experiments to not only verify the left-handed properties but also to evaluate the performance of the material. The experiments are usually carried out for power transmission, prism refraction, beam shifting and focusing. In most cases, we use an HP8350B with a plug-in option HP83592A as EM wave source, which can output 20 MHz to 20 GHz microwave power of up to 17 dBm at a fixed frequency or 15 dBm in frequency sweep scanning. The source is modulated by a 28.8 KHz square wave to cooperate with a scalar network analyzer HP8756A. The above source and network analyzer are of the same types as those used in [2]. The detector is an HP11664A.

2.1. Obtaining Non-Normalized Plane Wave

The first step to perform our measurements on left-handed materials is to obtain a proper incident beam for the experimental setup. In most cases, a plane wave is the ideal input to evaluate the properties of left-handed materials. In an experimental configuration, we therefore need to eliminate intereferences from the environment as much as possible. As has been used in [2], we also utilize a parallel plate waveguide (PPW) with microwave absorber on the two lateral sides to generate

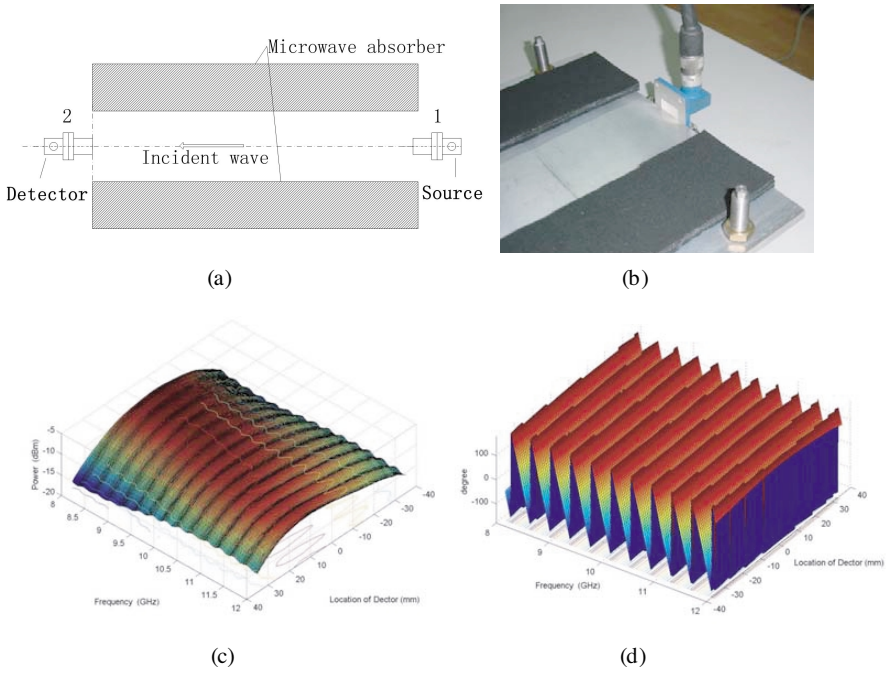

Figure 1. Method to generate plane wave.

a non- normalized plane wave. Figure 1(a) shows a brief scheme of the setup, in which the 3-cm rectangular waveguide adaptor 1 serves as the source and the adaptor 2 serves as the detector. Figure 1(b) shows the coupling method of the source, such that TE01 mode is fed into the PPW chamber. Figure 1(c) and 1(d) show the amplitude and phase of the output EM wave, indicating that at each frequency, the output EM beam is indeed a non-normalized plane wave, and its amplitude distribution is similar to a Gaussian beam.

2.2. Power Transmission Experiment

Figure 2 shows the experimental setup for the measurement of power transmission through a slab of metamaterial. Simulations and experiments of the power transmission property of a possible left-handed metamaterial is a basic but useful way to calibrate the dimensions of the structure and verify its LH properties. In the simulation, by observing the "backward" phase propagation, we can ensure the left-handed status and hence determine the dimensions of

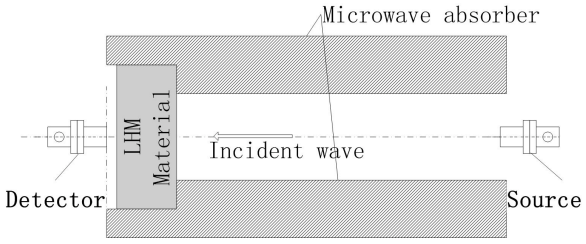

Figure 2. Experimental setup for the measurement of power transmission property.

the SRRs, rods and unit cell as well as the dielectric constant of the substrate. Following this step, the real power transmission results can be used to verify the simulation results, and to evaluate the insertion losses and the frequency bandwidth over which left-handness occurs.

2.3. Prism Refraction Experiment

The prism experiment was first proposed in [2]. Figure 3(a) shows the diagram and Figure 3(b) the setup we realized precisely according to the description in [2]. Before the experiment, the empty setup and a Teflon prism are measured to callibrate the measurements and to ensure that all apparatuses work well. By observing if the refracted beam is bent on the same side of the normal as the incident beam, we can directly judge whether the sample exhibits left-handed

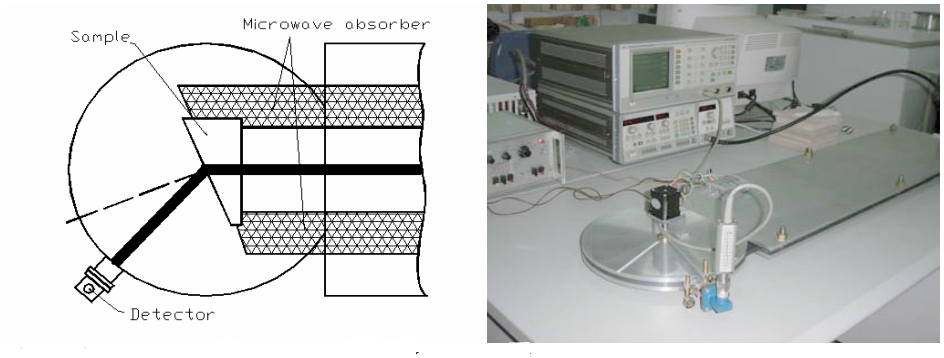

(a) (b)

Figure 3. Prism refraction experiment.

properties at the working frequency and estimate its effective index of refraction. The shortcoming of the prism experiment is that the beam transmitted through the triangular-shaped prism does not experience uniform losses, which influences the judgment of left-handed property when the losses of the sample are large or when the negative refractive angle is small [7]. This question could be solved by performing a beam shifting experiment, as we shall detail next.

2.4. Beam Shifting Experiment

The experimental setup for measuring the additional shift of a beam after transmitting through a slab-shaped sample [8–10] is depicted in Figure 4. A parallelogram-shaped slab, which could be regarded as two combined prisms as described in the previous section, is placed in the PPW chamber. In this case refraction occurs twice at the interfaces of the slab and the air [9, 10]. The beam shifts by a quantity d given by

$$d = w \sin\theta_1 \cos\theta_1 \left(1 - \frac{\cos\theta_1}{n_2 \sqrt{1 - \left(\frac{\sin\theta_1}{n_2} \right)^2}} \right) \tag{1}$$

where n_2 represents the refraction index of the slab and θ_1, θ_2 represent the incident and refraction angles, respectively. It is easy to see that there exists a maximum value of the shift for a slab of material which is not a left-handed, namely

$$d_{\max} = w \cos\theta_1 \sin\theta_1 \tag{2}$$

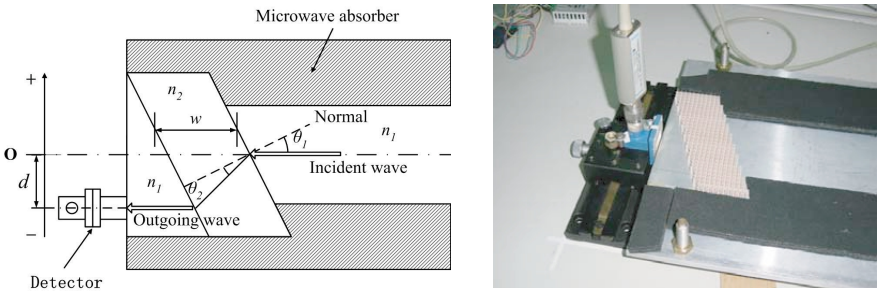

(a) (b)

Figure 4. Beam shifting experiment.

Hence, if the width w and incident angle θ_1 are known, the property (left-handed or right-handed) of the sample can be known by simply examining whether the beam shift is larger or smaller than $d_{\max}$ [10]. In the experiment, two or more measurements should be performed to ensure the precision: one is performed after the sample is removed to get the reference point O, another is performed when the sample is placed in to get the beam shift d. Obviously, the refractive index can also be calculated by virtue of (1) after d is measured.

Compared with the prism experiment, when the beam is transmitted through the parallelogram-shaped sample, the loss is uniform everywhere and the results are then more reliable.

2.5. Focusing Experiment Using One Dimensional Sample and Radiate Source

Lenses may be one of the most promising applications of left-handed materials. Figure 5 shows the experimental setup for observing the focusing of a radiate EM wave by a one dimensional sample. A monopole is placed at the center of a PPW consisting of two parallel circular Aluminum plates. The backward transmitted wave is dissipated by the microwave absorbers, and the forward transmitted wave is measured by the detector along the circular edges of the plates. By measuring and comparing the width of the output beam before and after a sample of left-handed material is placed in front of the antenna, we can observe if the LH slab can focus a radiation pattern. A similar experimental setup could also be used to observe the radiation pattern sharpening by a slab of left-handed material, in which the monopole is placed in the middle or touching the side edge of the slab, and to observe if the main lobe of the monopole is sharpened.

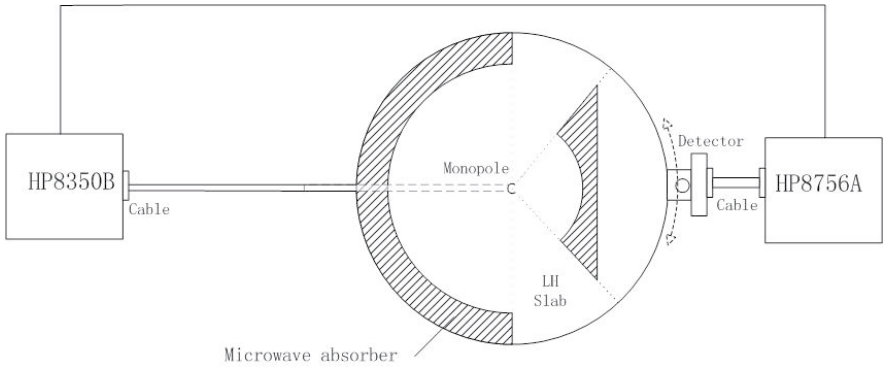

Figure 5. Radiation pattern sharpening experiment.

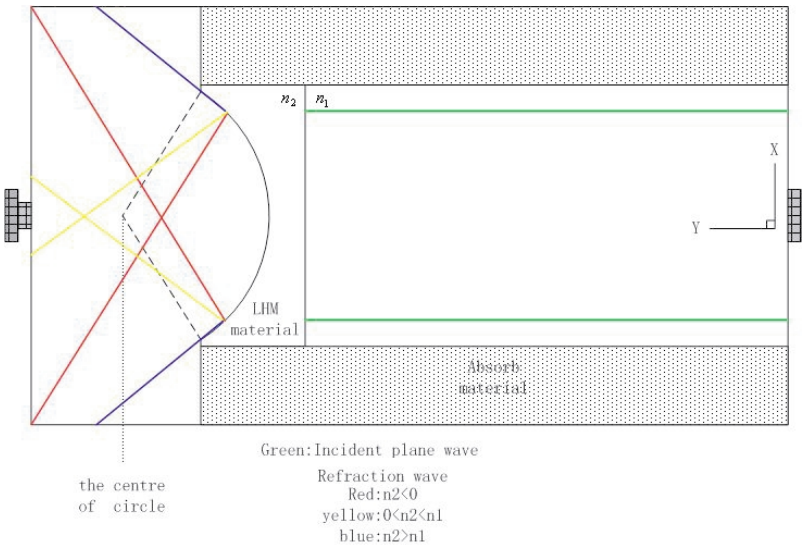

Figure 6. Focusing experiment using 1-D metamaterial sample.

2.6. Focusing Experiment Using One Dimensional Sample and Plane Wave Source

In [5], a focusing experiment is performed using a slab-shaped sample and a radiate source, which is suitable for a 2-D isotropic metamaterial. However, when testing a 1-D metamaterial, the setup of Figure 6 can be adopted. In this case, a special shaped sample (a half concave lens with a circular edge) and a plane wave source are used. Since the refraction occurs at the curved interface, an input plane wave with proper polarization meets the working conditions of a one dimensional metamaterial. After a simple analysis we see that, if the refractive index of the sample is negative, the focus will be located in the range enclosed in the curved interface and the dashed lines. If the refractive index of the sample is positive, the focus will be located beyond the dashed lines. This experiment is an equivalent to the slab focusing one.

3. EXPERIMENTS

In this section, we introduce three types of left-handed materials: a symmetric ring structure, an Ω-like resonator structure and an S-shaped resonator structure.

3.1. Symmetric Ring Structure

3.1.1. Structure and Dimensions

Figure 7(a) and (b) show the configuration of split-ring resonator, which was initially used at infrared frequencies [11] and which has been adapted to microwave frequencies. Compared with the SRRs/rods configurations in [6], two rings of this particular structure now have

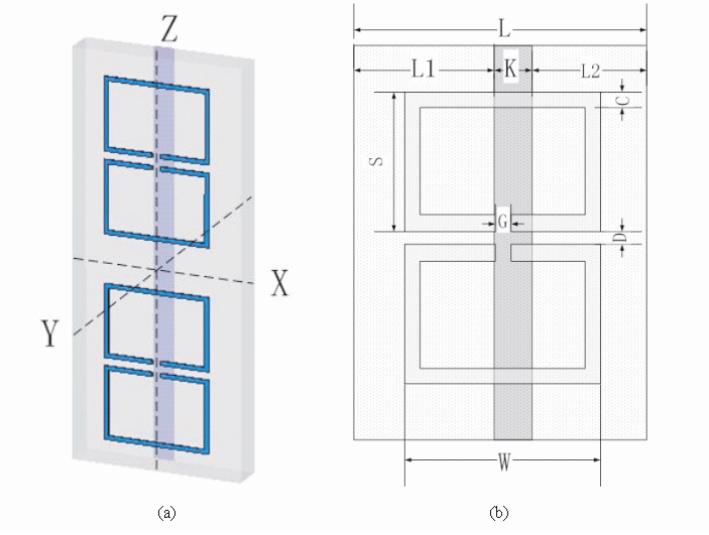

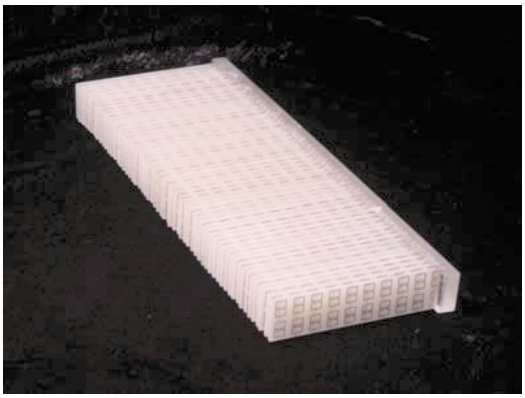

(c)

Figure 7. Dimensions of the symmetric ring structure and the photograph of a realized slab.

the same size and are symmetric with each other. In our realization, the related dimensions are: $L = 5.04\,\text{mm}$, $L1 = 2.4\,\text{mm}$, $L2 = 2.04\,\text{mm}$, $K = 0.6\,\text{mm}$, $C = 0.24\,\text{mm}$, $D = 0.24\,\text{mm}$, $G = 0.24\,\text{mm}$, $W = 3.12\,\text{mm}$, and the dielectric constant of the substrate is about 4.6. The rod is placed on the opposite side of the substrate, and has a length of 12 mm. Figure 7(c) shows a physically realized 1-D slab consisting of 10×60 unit cells. The substrate is 1-mm-thick FR4-type PC board. All the PC boards are pasted on a frame with a lot of slots, which is made of organic plastic.

3.1.2. Power Transmission Property

Figure 8(a) shows the experimental results of a SRRs only slab, in which the rods array has been removed in order to observe the forbidden band induced by the negative permeability. We see that, there indeed exists a forbidden gap at about 8 GHz to 9 GHz. The rising edge at about 6.5 GHz corresponds to the cut-off frequency introduced by the 3-cm waveguide adaptator used in the setup. The forbidden band is in agreement with Figure 8(b), which is a simulation result for a 1-D slab consisting of 8×18 of the aforementioned SRRs unit cells. The "backward" phase propagating direction can be clearly observed in the simulation.

3.1.3. Prism Refraction Experiment

To further confirm that the metamaterial is indeed left-handed in this frequency band, we performed a Snell refraction experiment using a prism-like sample. The shape of the prism and the experimental setup are the same as those in [2]. Figure 9 shows the 3D plot of the experimental results. We see clearly that, in the frequency band of about 8.2 GHz to 8.7 GHz, there is a stand alone negative peak, which corresponds to a refraction direction of about -30 degrees, corresponding to a negative index range of 0 to -2. This result is also in agreement with the simulations.

3.1.4. Beam Shifting Experiment

Figure 10 shows the result of the beam shift experiment. In the corresponding frequency band, the beam is shifted to the negative direction, and the center of the beam is located at $-34\,\text{mm}$. The measurements of the empty setup show that the reference point O is located at $-13\,\text{mm}$, therefore the net beam shift is then $-21\,\text{mm}$, corresponding to a refractive index of about -2. The measurements of the Teflon show that the center of the beam is located at $-16\,\text{mm}$,

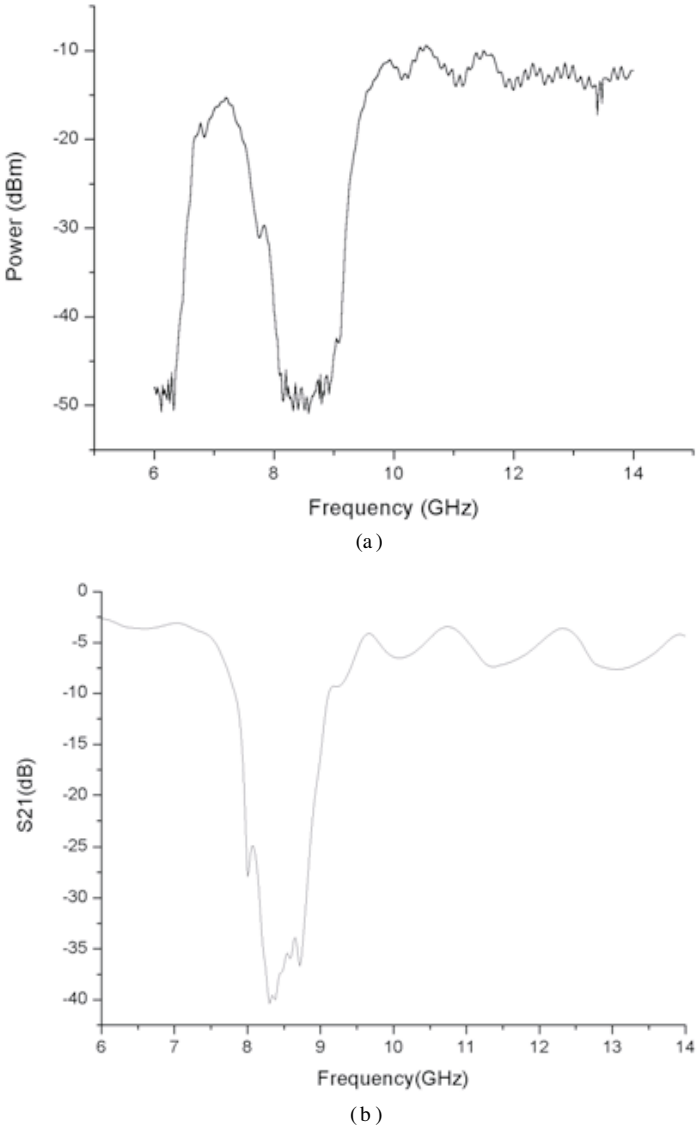

Figure 8. Power transmission property of SRRs only slab.

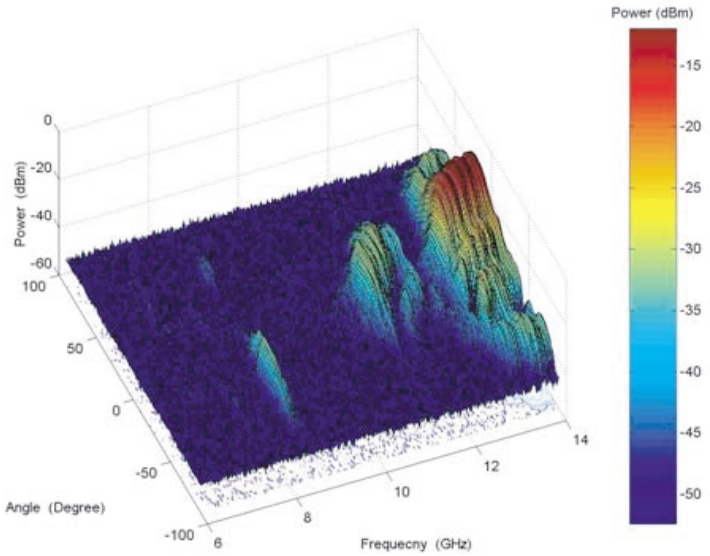

Figure 9. Prism experimental result for the symmetric ring structure.

corresponding to a refractive index of about 1.5. Although the beam shift experiment is not ideal for a one dimensional sample, the left-handed phenomenon can still be observed.

3.1.5. Focusing Experiment

Figure 11 shows the setup for observing the focusing phenomenon for 1-D left-handed material in the case of plane wave incidence. The receiver port is driven to move in the X direction (see Figure 6) by a motor, and the metamaterial is moved by hand in the Y direction.

Figure 12(a) shows the results for an operating frequency of 10 GHz, at which the metamaterial is still a right-handed material. Figure 12(b) shows the results at 8.4 GHz, where the metamaterial should be left-handed, according to our previous prism and power transmission experiments. Compared with Figures 12(a) and (b) we see that of 8.4 GHz the beam behaves like an expanded beam after being transmitted through the metamaterial and in agreement with the red line in Figure 1. However, the measurement resolution of the experiment is not adequate. The continued experiment is still in preparation.

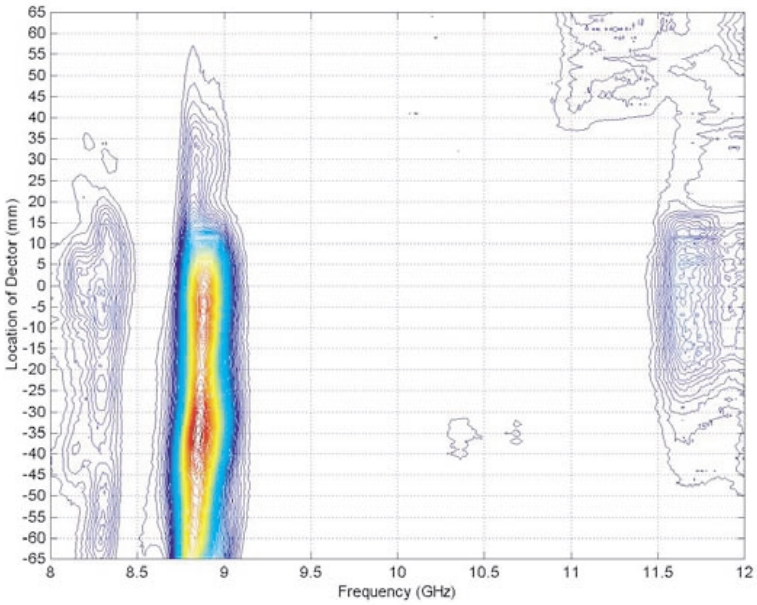

Figure 10. Beamshifting experimental result for the symmetric ring structure.

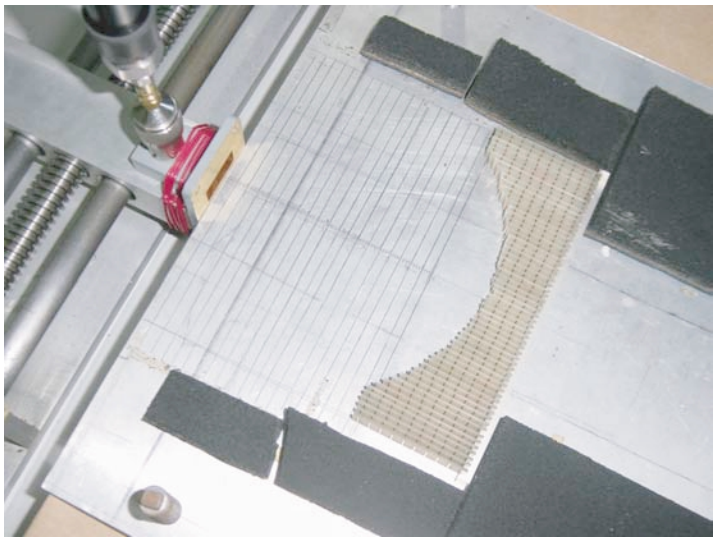

Figure 11. Focusing experiment for the 1-D sample.

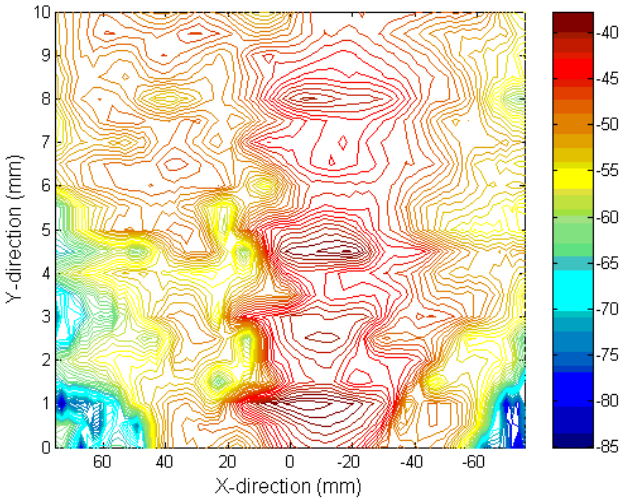

(a)

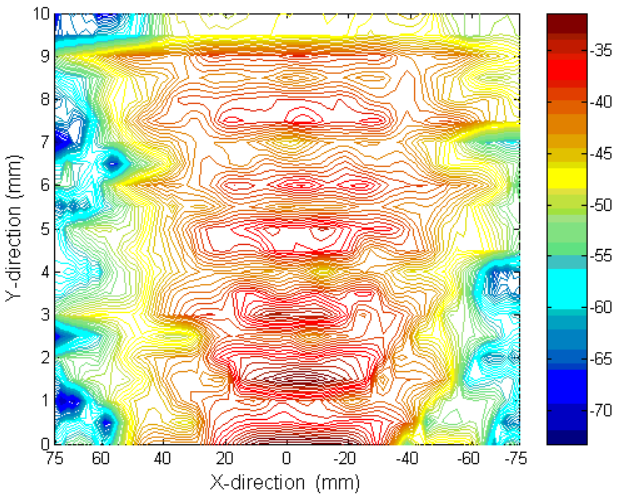

(b)

Figure 12. Experimental results of focusing experiment at 10 GHz (a) and 8.4 GHz (b).

3.2. Ω-like Resonator Structure

In this section, we introduce another configuration of left-handed material, which is fabricated by Ω-like metallic patterns and circuit board substrates. In 1992, M. M. I. Saadoun and N. Engheta introduced the concept of "Ω media", which could be regarded as a "pseudochiral" or bianisotropic [13]. C. R. Simovski et al. recently concluded that such perfectly conducting Ω-shape "particles" could also be used to construct LH metamaterials [14]. Our realization of Ω media is based on stacked Ω-like metallic patterns and repeated periodically [15]. Experimental results show that this configuration has better performance. Further, as it shall be seen in the next section, such a structure can be compressed using hot-compress techniques into a solid-state-like material with reduced losses.

3.2.1. Structure and Dimensions

Figure 13 shows the dimensions of the basic unit cells and the photograph of the finished anisotropic metamaterial in which three Ωs are stacked in series to form a basic unit. Two such units are placed oppositely and closely in order to increase the coupling and avoid chiral effects. Figure 13(a) shows the basic unit cells of the Ω-like structure

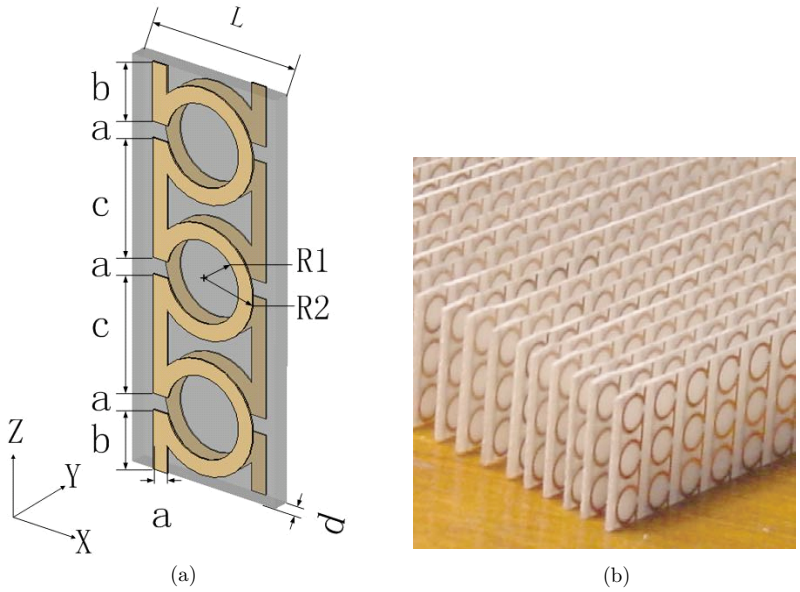

Figure 13. Dimensions and realization of Omega media.

with dimensions designated as $a, b, c, R1$ and $R2$. For the experimental setup we have $a = 0.4\,\text{mm}$, $b = 1.5\,\text{mm}$, $c = 2.9\,\text{mm}$, $R1 = 1\,\text{mm}$ and $R2 = 1.4$. Three Ωs are conected in series to form the basic unit, and a number of such units are placed side by side with a distance of $d = 4\,\text{mm}$. The Ωs are printed on both sides of an FR4-type PCB substrate with a thickness of 0.4 mm. Placing many pieces of this type of PC board side by side at a distance of 2.5 mm forms a rectangular metamaterial.

3.2.2. Power Transmission Property

Figure 14 shows the experimental and simulation results of power transmission through a metamaterial slab consisting of 10×80 unit cells along x and y directions (see Figure 14), respectively. The beam is incident from the x direction. The slab is placed between two aluminum plates with microwave absorbers on the sides, yielding a similar experimental setup as the one in [16]. Figure 14(b) shows the experimental results. We clearly see that there is a pass band located from 12 GHz to 13.2 GHz. The frequency corresponding to the peak value of the power is 12.6 GHz, related to a wavelength (in the air) of about 24 mm. Therefore, the repeated length of the unit cell in x (4 mm) and z (3.4 mm) directions are one sixth or less of the wavelength and therefore the slab can be regarded as an approximately homogeneous material at these frequencies. Figure 14(a) shows the simulation results of the same structure. The simulation environment is similar to the experimental setup. There also exists a pass band between 12 GHz and 13 GHz. We see that the experimental results agree well with the simulated ones.

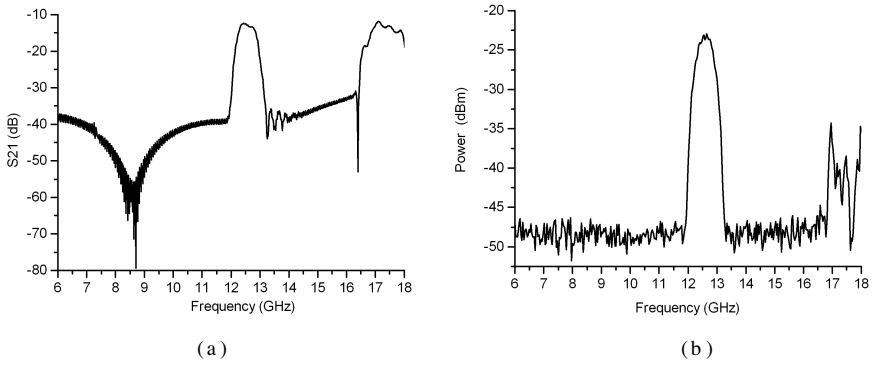

Figure 14. Power transmission characteristics. (a) Simulation result. (b) Experimental result.

3.2.3. Prism Refraction Experiment

Figure 15 shows the result of the Snell refraction experiment, in which the experimental setup is similar to the one described in Figure 2 in [2]. Since the size of the basic unit cell in our metamaterial is shorter than that in [2] (4 mm × 2.5 mm vs. 5 mm × 5 mm), the angle of the hypotenuse and the longer side of the triangular prism is about 15.46°, instead of 18.43° in [2]. When an incident beam is introduced along the x direction, the incident angle at the hypotenuse edge is then also 15.46°. Another important difference is that, in our experimental setup, the distance between the two aluminum plates is 10 mm, indentical to the height of the prism. This means that the two sides of the prism contact with the plates. However, this does not mean that all the "arms" of the Ωs are well electrically connected with the plates.

Figure 15(a) shows the 3-D result of the experiment. We see that there is a "negative" peak located around 12.6 GHz. The LH band is up to 1.2 GHz, and agrees exactly with the pass band in the power transmission experiment. The loss of the prism at 12.6 GHz is smaller than −14 dB, which is much less than the previous losses recorded. Figure 15(b) shows a 2-D power-frequency plane extracted from Figure 15(a) at 12.6 GHz. From this plane, we see that the refracted beam is bent at an angle about −27°, corresponding to an effective index of refraction of about −1.7.

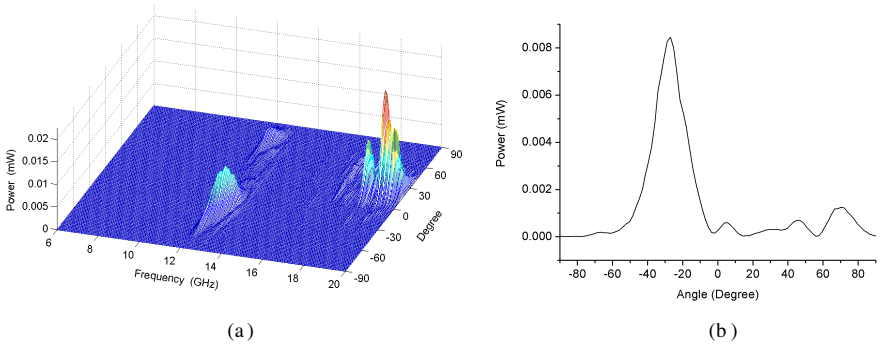

Figure 15. Snell refraction experimental results. (a) 3-D result with the three axes representing detected power in mW, frequency in GHz and angle in degree, respectively. (b) 2-D curve extracted from the 3-D result at 12.6 GHz.

Figure 16 shows the curve of the refractive index versus frequency. We see that in the pass band from 12 GHz to 13.2 GHz, the index value is negative, indicating that the "negative" band of the metamaterial

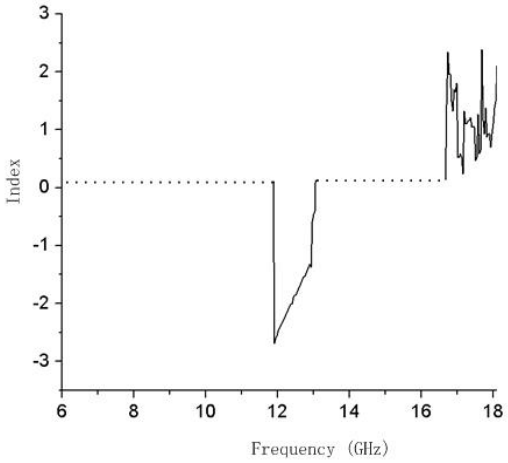

Figure 16. Refractive index of the metamaterial. This curve is calculated from Figure 3. The frequency bands of 6 GHz to 12 GHz and 13.2 GHz to 16.5 GHz correspond to two stop bands, which are represented by dashed lines. In the band of about 12 GHz to 13.2 GHz, the refractive index is negative.

extends up to 1.2 GHz. Furthermore, our simulations demonstrate that if the electrical contact of the "arms" of the Ωs and the parallel plates is improved, we can get a wider negative band and less losses. On the contrary, the negative band is decreased and the loss is increased when we slightly lift-up the top plate of the planar waveguide.

3.2.4. Focusing Experiment

In order to observe the focusing phenomenon by a one dimensional sample, the system described in Figure 5 is setup. A monopole is located at the center of the circular plate and serves as a radiating source. We know that the radiation pattern of the magnetic field has also a circular form. The Ω boards are disposed in a radial manner to fit the incident EM wave. The setup is shown in Figure 17, and the measured results are shown in Figure 18. Within the frequency band of 12 to 14 GHz, we clearly see a stand alone peak, which corresponds to a focus of the original source, although it might not be the focus itself. Further two dimensional measurement are in preparing to observe a full image of the focusing procedure. Also we have tried to observe the radiation pattern sharpening phenomenon by replacing the special sample by a slab and placing the sample in touch with the antenna.

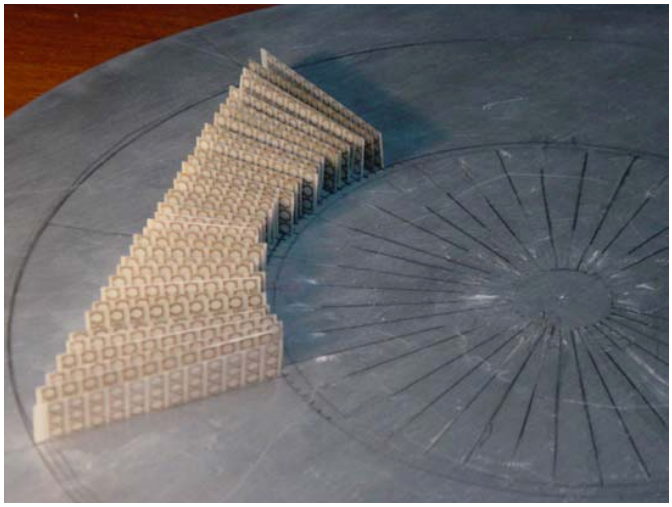

Figure 17. A new shape so that the antenna(s) could be placed in the center of the circular plate.

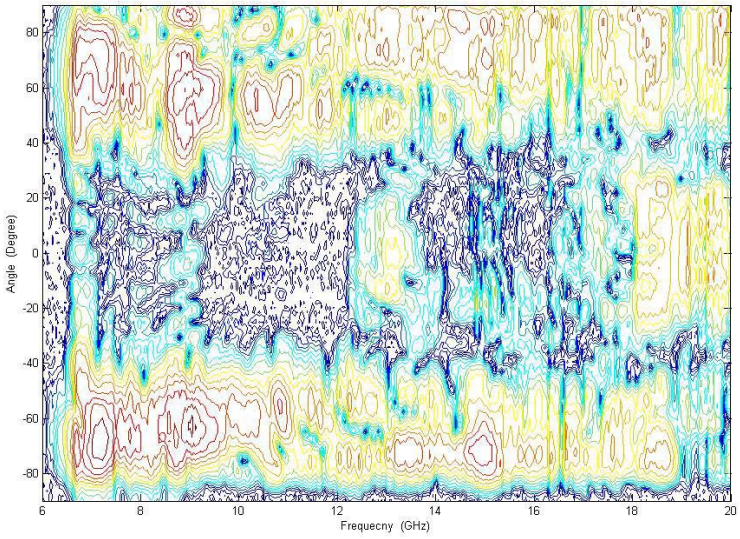

Figure 18. Experimental results correspond to Figure 17.

Although we see the sharpening, we do not publish the data, because the measurement is not strictly in far field.

3.3. Solid-State Multi-Layer Omega-Like Structure

3.3.1. Structure, Dimensions and Hot-Pressure Technique

Figure 19 shows the diagram for the production of a one-dimensional multi-layer left-handed solid-state material. The hot-press technique is a standard technic used in the manufacture of multi-layer printed circuit boards. Here we use this technique to compress the PC boards with and without metallic patterns together under high temperature and press to obtain a left-handed material of solid-state form. The material thus produced has more stable and better characteristics, both

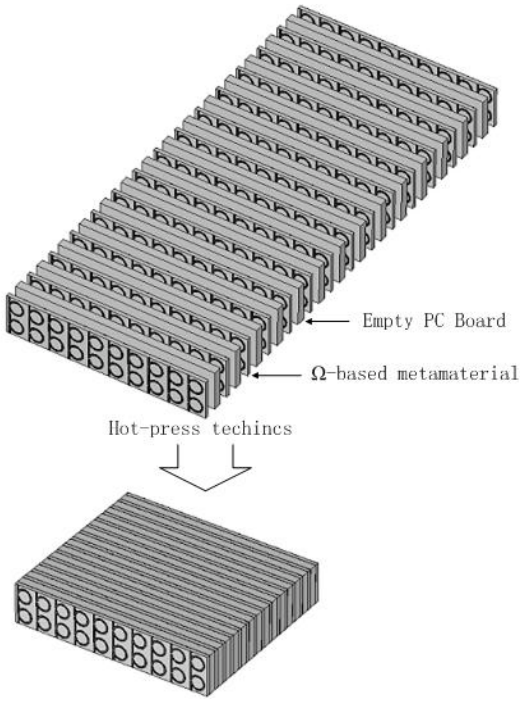

Figure 19. Diagram of fabricating solid-state bianisotropic LH metamaterial. The upper part shows pieces of Ω-based metamaterial and empty PC board substrates. By compressing them together, we can get a solid state metamaterial, which has more stable LH properties and is easier to be used in experiments and other possible applications.

from a mechanical standpoint and an electromagnetic standpoint.

We use two series-stacked Ω-like metallic patterns to serve as the basic resonator unit to be printed on a PC board. Applying the hot-press technique mentioned above, we produce a solid-state metamaterial sample by compressing pieces of alternately stacked PC boards with and without Ω patterns. The inner and outer radii of the Ω pattern are 1.5 mm and 1.9 mm, respectively. The length of the arm of the Ω is 2.3 mm. The gap between the two arms is 0.4 mm. The width of the printed track is also 0.4 mm. The Ω patterns are printed on both sides of a 1-mm-thick standard PC board substrate with reversed orientations in order to cancel chiral effects [14]. Each unit cell occupies a 5-mm space. The boards without Ω patterns have the same permittivity value as that printed with Ω patterns. The pieces of the PC boards with and without Ω patterns are stacked and compressed under a temperature above 380°C and a initial pressure above 4 tons. Figure 20 shows the machine used to hot-compress the samples and the photograph of original compressed sample. Figure 21 shows a piece of sample we used in the following experiments.

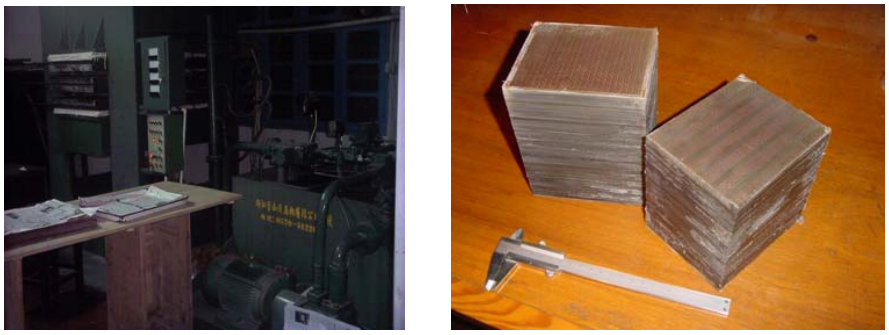

(a) (b)

Figure 20. Producing solid-state omega media.

3.3.2. Power Transmission Experiment

In Fig. 22, the curve corresponding to the transmission property of a metamaterial slab is represented by a solid line and has a passband with a center frequency at 8.85 GHz and a bandwidth close to 1 GHz. The detected peak value is −14.8 dBm at 8.85 GHz. In order to estimate the insertion losses of the metamaterial slab, we measure the transmission power in the same experimental setup after the metamaterial slab is removed. The corresponding value at 8.85 GHz is −9.8 dBm, which

Figure 21. The solid-state omega sample used in the experiments.

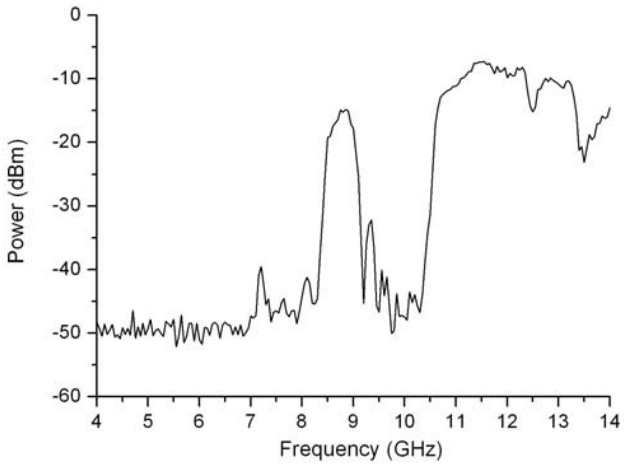

Figure 22. Power transmission property of the solid-state sample.

can be approximated as the power incident upon the interface of the slab and air. Thus, with a return loss at the incident interface, the maximum insertion loss of the slab composed of 10 unit cells is less than 5 dB, which corresponds to less than 0.5 dB/unit cell.

3.3.3. Prism Experiment

Fig. 23 shows the experimental results of the prism refraction experiment, in which the horizontal axis represents frequency, the vertical axis represents the refraction angle, and the contour lines

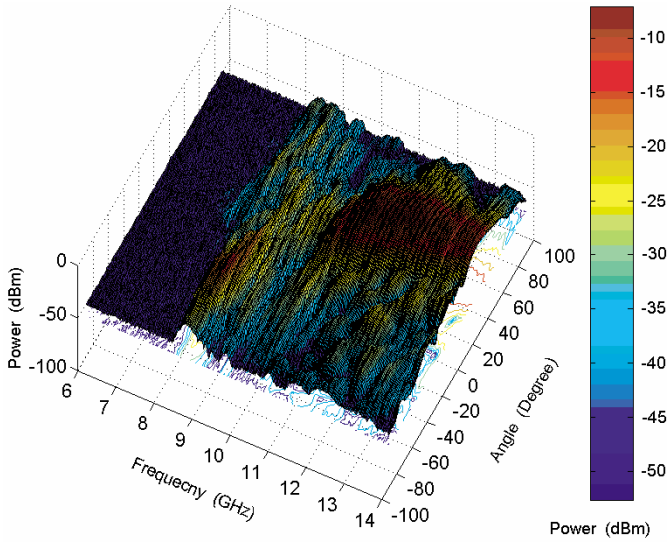

Figure 23. Negative refraction of the solid-state Omega sample.

represent the detected power in dBm. In the experiment, the setup is the same as that described in [2], and also has been tested with a Teflon sample. We see that the frequency band bellow 8 GHz is a stopband, where only noise power can be detected. The frequency band from 8.3 GHz to 9.3 GHz shows a clear left-handed behavior, in which the beam is bent toward negative angles. Again, in this area, small losses are observed.

3.3.4. Beam Shifting Experiment

The principle of the beam shifting experiment has already been exposed in Section 2.4. We report in Fig. 24 the results with the solid state metamaterial. The experiment is performed in a planar waveguide with microwave absorbers on the two sides. The metamaterial sample, as well as a Teflon sample, are cut into a shape of parallelogram. The thickness of the slab is 5 cm and the incidence angle is about 18.4 degrees. A beam shift exceeding the location of -15 mm ensures that the slab consists of a left-handed material. Fig. 24 shows the beam centers (determined from the peak value) in the cases of air, Teflon, and the metamaterial sample. The centers are located at 1 mm, -3 mm, and -23 mm, respectively, demonstrating that the metamaterial sample is indeed a left-handed medium.

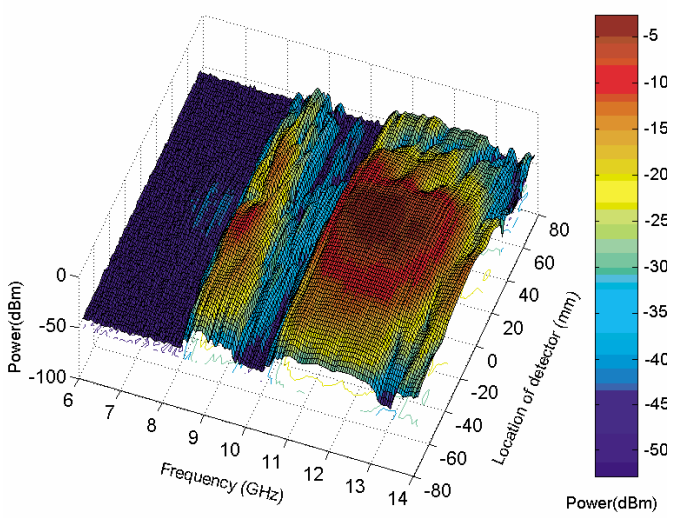

Figure 24. Beam shift experimental results of the solid-state Omega sample.

3.4. *S*-Shaped SRR Structure

In this section we study a metamaterial structure which is composed of a series of *S*-shaped resonators [17] connected with each other. Such a metamaterial has been shown to exhibit low losses and a left-handed behavior over a large frequency band. A sample of the metamaterial is shown in Fig. 25 and a prism-like sample is cut for the beam refraction experiment. The three dimensional results of the beam refraction experiment are shown in Fig. 26, where we clearly see that it has a wide frequency band of negative refraction, about 2.6 GHz, from 10.9 GHz to 13.5 GHz.

4. EQUIVALENT CIRCUIT ANALYSIS

In the study of various SRRs, we have found that all the configurations of SRR proposed in the literatures [2, 11, 12, 18] can be modeled as a general equivalent circuit, from which the effective permeability of the SRR structures can be calculated. A more complicated structure like the newly proposed Ω-like metamaterial [13], as shown in Fig. 27(a, b) still can be modeled as an equivalent circuit, as shown in Fig. 27(c),

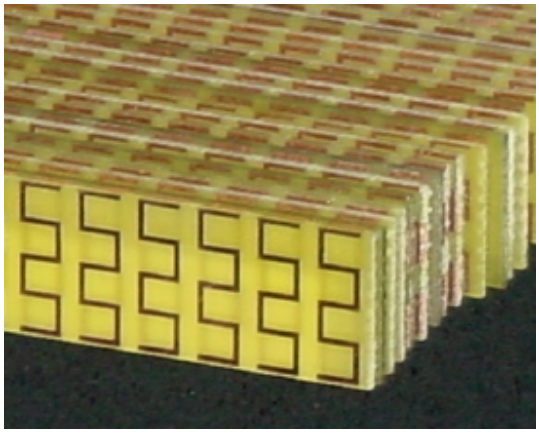

Figure 25. Metamaterial composed of 'S'-shaped SRR.

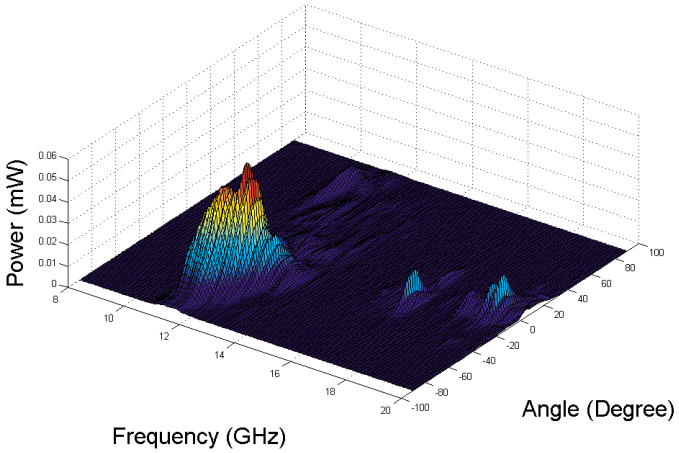

Figure 26. 3-D illustration of the beam refraction experiment result. The metamaterial exhibits a negative refraction over the frequency range from 10.9 GHz to 13.5 GHz.

and the effective permeability can be calculated to be

$$\mu_{eff} = 1 - \frac{(F_1 + F_2)\left\{\omega^2 - \omega_{m0}^2 \left(\dfrac{F_1 - F_2}{F_1 + F_2}\right)^2\right\} + iW'(\sigma)}{\omega^2 - \omega_{m0}^2 + iX'(\sigma)} \tag{3}$$

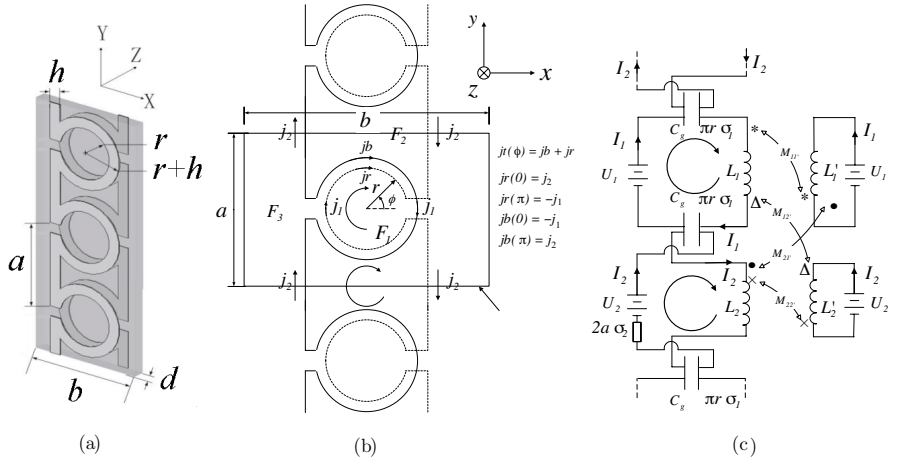

Figure 27. Fig. 27(a) Omega-like metamaterial [7]. The Omega-like structures are printed on both sides of a substrate with reversed orientations. The width of the circular ring is h, and the thickness of the substrate is d. The dimensions of a unit cell are a in the y direction, b in the x direction, and l in the z direction. (b) Omega-like metamaterial in xy plane. The solid line indicates the front Omega, and the dashed line indicates the omega in opposite side. The rectangular sketched means a unit cell of such periodic structure. So $S = ab$ is the total area of a unit cell in xy plane. The conductors of the Omega structure divided the unit cell into three parts: $F_1 = \frac{\pi r^2}{S}$ is the fractional volume of the cell occupied by the interior of the circular rings (Area I), $F_2 = \frac{2ra-\pi r^2}{S}$ is the fractional volume of the cell enclosed by the two arms of the omega but external to the rings (Area II), and $F_3 = \frac{ab-2ra}{S}$ is the fractional volume of the cell not enclosed by the arms (Area III). Currents flow around the two loops under magnetic induction. (c) Equivalent circuit model of the Omega-like metamaterial. C_g is the capacitance between the two sheets of the half circular ring in a unit length of z, σ_1, σ_2 are the resistance per unit length in each loop with unit of ohm/m. U_1, U_2 are the sources in the two loops that induced by the external field H_0. L_1, L_2 are the inductance in the two loops, respectively. L_1', L_2' are the total inductances of Loop 1 and Loop 2 in other units, respectively. And $M_{11'}$, $M_{22'}$, $M_{12'}$ and $M_{21'}$ are the mutual inductances between L_1, L_2, L_1', and L_2'.

where

$$\begin{aligned} C &= C_g/2 \\ L_1 &= \mu_0 F_1 S/l \\ L_2 &= \mu_0 F_2 S/l \end{aligned} \tag{4}$$

and $W'(\sigma)$, $X'(\sigma)$ are the loss components.

If we take the following values:

$$\begin{aligned} &a = b = 5 \times 10^{-3}\,\mathrm{m} \\ &r = 1.5 \times 10^{-3}\,\mathrm{m} \\ &h = 0.5 \times 10^{-3}\,\mathrm{m} \\ &d = 0.1 \times 10^{-3}\,\mathrm{m} \\ &l = 2.5 \times 10^{-3}\,\mathrm{m} \\ &\sigma_1 = 0.1 \\ &\sigma_2 = 0.1 \end{aligned} \tag{5}$$

we can calculate the effective permeability as shown in Fig. 28.

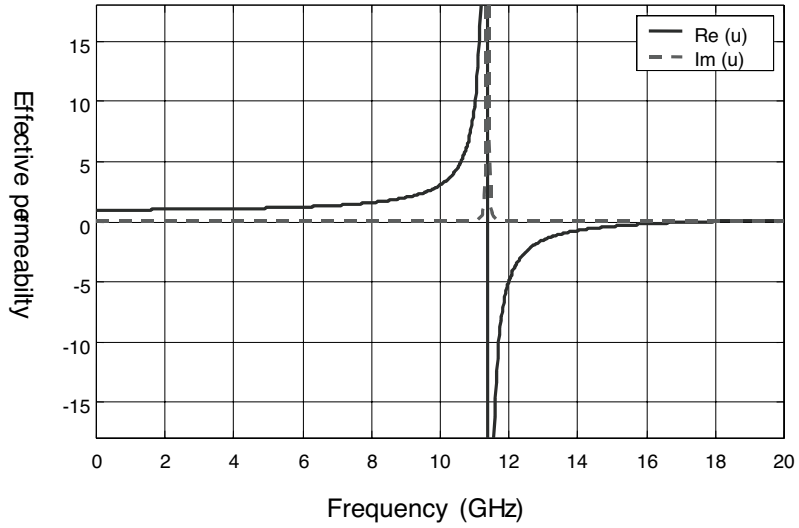

Figure 28. Effective permeability of omega structure with $\sigma_1 = 0.1, \sigma_2 = 0.1$.

5. CONCLUSION

In this paper, we have reported experimental results obtained by measuring several types of left-handed metamaterials. By using different experiments and different shapes of samples, we have verified that these samples do exhibit LH properties. Through the above experiments, we conclude that the metamaterials samples constructed by Ω-like metallic patterns and S-shaped resonators, in solid-state form, exhibit a clear left-handed behavior in a wide frequency band and with very low losses, and have other stable electromagnetic and mechanical characteristics. From the solid-state form, we can cut the metamaterials into various shapes, plate metallic films on their surfaces, and fix or install them into a device package. The insertion losses of a solid-state Ω slab medium consisting of 5 unit cells are smaller than 2.5 dB, which is smaller than those of many microwave devices. Thus it is now possible to use this material to produce various microwave devices.

ACKNOWLEDGMENT

This work is supported or partly supported by Chinese Natural Science Foundation under items No. 60371010, 60201001 and 60271010.

REFERENCES

1. Veselago, V. G., "The electrodynamics of substances with simultaneously negative values of ε and μ," *Sov. Phys. Usp.,* Vol. 10, No. 4, 509–514, 1968.
2. Shelby, R. A., D. R. Smith, and S. Schultz, "Experimental verification of a negative index of refraction," *Science,* Vol. 292, No. 6, 77–79, 2001.
3. Pendry, J. B., "Negative refraction makes a perfect lens," *Phys. Rev. Lett.,* Vol. 85, No. 18, 3966–3969, 2000.
4. Engheta, N., "An idea for thin subwavelength cavity resonators using metamaterials with negative permittivity and permeability," *IEEE Antennas and Wireless Propagation Letters,* Vol. 1, No. 1, 10–13, 2002.
5. Enoch, S., G. Tayeb, P. Sabouroux, N. Guérin, and P. Vincent, "A metamaterial for directive emission," *Phys. Rev. Lett.,* Vol. 89, No. 18, 213902:1–4, 2002.
6. Smith, D. R., W. J. Padilla, D. C. Vier, S. C. Nemat-Nasser, and S. Schultz, "Composite medium with simultaneously negative

permeability and permittivity," *Phys. Rev. Lett.,* Vol. 84, No. 18, 4184–4187, 2000.

7. Sanz, M., A. C. Papageorgopoulos, W. F. Egelhoff, Jr., M. Nieto-Vesperinas, and N. Garcia, "Transmission measurements in wedge-shaped absorbing samples: an experiment for observing negative refraction," *Phys. Rev. E.,* Vol. 67, 067601:1–4, 2003.
8. Kong, J. A., "Electromagnetic waves in stratified negative isotropic media," *Progress in Electromagnetics Research,* PIER 35, 1–52, EMW Publishing, Massachusetts, 2002.
9. Kong, J. A., B. I. Wu, and Y. Zhang, "Lateral displacement of a Gaussian beam reflected from a grounded slab with negative permittivity and negative permeability," *Appl. Phys. Lett.,* Vol. 80, No. 12, 2084–2086, 2002.
10. Ran, L., J. Huangfu, H. Chen, X. Zhang, K. Chen, T. M. Grzegorczyk, and J. A. Kong, "Beam shifting experiment for the characterization of left-handed properties," *J. Appl. Phys.,* Vol. 95, No. 5, 2004.
11. O'Brien, S. and J. B. Pendry, "Magnetic activity at infrared frequencies in structured metallic photonic crystals," *J. Phys: Condens. Matter 14,* 6383–6394, 2002.
12. Grzegorczyk, T. M., C. D. Moss, J. Lu, X. Chen, J. P. Pacheco Jr., and J. A. Kong, "Properties of left-handed metamaterials: transmission, backward phase, negative refraction, and focusing," submitted to *MTT*, 2005.
13. Saadourn, M. M. I. and N. Engheta, *Microwave Opt. Technol. Lett. 5,* 184, 1992.
14. Simovski, C. R. and S. He, *Phys. Lett. A 311,* 254, 2003.
15. Huangfu, J., L. Ran, H. Chen, X. Zhang, K. Chen, T. M. Grzegorczyk, and J. A. Kong, "Experimental confirmation of negative refractive index of metamaterial composed of W-like metallic patterns," *Appl. Phys. Lett.,* Vol. 84, No. 9, 2004.
16. Shelby, R. A., D. R. Smith, S. C. Nemat-Nasser, and S. Schultz, "Microwave transmission through a two-dimensional, isotropic, left-handed metamaterial," *Appl. Phys. Lett.,* Vol. 78, No. 4, 489–491, 2001.
17. Chen, H., L. Ran, J. Huangfu, X. Zhang, K. Chen, T. M. Grzegorczyk, and J. A. Kong, "Left-handed material composed of only S-shaped resonators," submitted.
18. Pendry, J. B., A. J. Holden, D. J. Robbins, and W. J. Stewart, "Magnetism from conductors and enhanced nonlinear phenomena," *IEEE Trans. Microwave Theory Tech.,* Vol. 47, No. 11,

2075–2084, 1999.

Lixin Ran was born in P. R. China in 1968. He received the Bachelar, Master and Ph.D. degrees from the Department of Information and Electronic Engineering of Zhejiang University in 1991, 1994 and 1997, respectively. He is currently an associate professor of Zhejiang University. His research interests involve the microwave circuits and chaos, left-handed materials, and high-speed digital circuits.

Jiangtao Huangfu was born in Henan, China, in 1978. He received the B.S. degree in information science and electrical engineering department from Zhejiang University, China, in 1999. He is currently working toward the Ph.D. degree at Zhejiang University. His current research interests include the left-handed material and the wireless communication.

Hongsheng Chen was born in Zhejiang, China, in 1979. He received the B.S. degree in information science and electrical engineering department from Zhejiang University, China, in 2000. He is currently working toward the Ph.D. degree at Zhejiang University. His current research interests include the application of the left-handed material, design wide-band low-loss metamaterial structures and numerical studies on electromagnetic properties of the metamaterial.

Xianmin Zhang was born in Zhejiang, China, in 1965. He received his B.S. and Ph.D. degrees in physical electronics and optoelectronics from Zhejiang University, China, in 1987 and 1992, respectively. He was appointed as an associate professor of information and electronic engineering at Zhejiang University in 1994 and full professor in 1999. He is currently the director of the Institute of Electronic Information Technology and System, Zhejiang University. His research interests include left-handed material, fiber optics, and microwave photonics.

Kangsheng Cheng is a professor of information and electronic engineering at Zhejiang University. From 1992 to 1996, he is the director of the information and electronic engineering department, Zhejiang University. From 1996 to 1999, he is the director of the personal office, Zhejiang University. His research interest is in the area of signal integrity, left-handed material, microwave and optical waveguide technology. He has published two books over 100 refereed articles.

Tomasz M. Grzegorczyk received his Ph.D. degree from the Laboratoire d'Electromagnétisme et d'Acoustique (LEMA), Ecole Polytechnique Fédérale de Lausanne (Swiss Federal Institute of Technology, Lausanne) in December 2000. His research activities concerned the modeling of millimeter and submillimeter structures using numerical methods, as well as their technological realizations with the use of micromachining techniques. In January 2001, he joined the Research Laboratory of Electronics (RLE), Massachusetts Institute of Technology (MIT), USA, where he is now a research scientist. His research interests include the study of wave propagation in complex media including left-handed metamaterials, the polarimetric study of ocean and forest, electromagnetic induction from spheroidal object for unexploded ordnances modeling, waveguide and antenna design, and wave propagation over rough terrains.

Jin Au Kong is a Professor of Electrical Engineering at the Massachusetts Institute of Technology. His research interest is in the area of electromagnetic wave theory and applications. He has published eight books, including Electromagnetic Wave Theory by Wiley Interscience, over 400 refereed articles and book chapters, and supervised over 120 theses. He is editor-in-chief of the Journal of Electromagnetic Waves and Applications, chief editor of the book series Progress in Electromagnetics Research, and editor of the Wiley Series in remote sensing.

HFSS视频培训课程推荐

HFSS 软件是当前最流行的微波无源器件和天线设计软件，易迪拓培训(www.edatop.com)是国内最专业的微波、射频和天线设计培训机构。

为帮助工程师能够更好、更快地学习掌握 HFSS 的设计应用，易迪拓培训特邀李明洋老师主讲了多套 HFSS 视频培训课程。李明洋老师具有丰富的工程设计经验，曾编著出版了《HFSS 电磁仿真设计应用详解》、《HFSS 天线设计》等多本 HFSS 专业图书。视频课程，专家讲解，直观易学，是您学习 HFSS 的最佳选择。

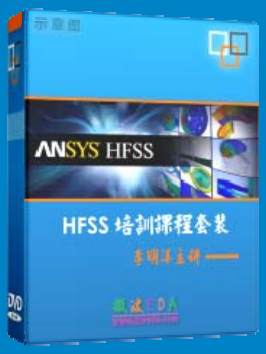

HFSS 学习培训课程套装

该套课程套装包含了本站全部 HFSS 培训课程，是迄今国内最全面、最专业的 HFSS 培训教程套装，可以帮助您从零开始，全面深入学习 HFSS 的各项功能和在多个方面的工程应用。购买套装，更可超值赠送 3 个月免费学习答疑，随时解答您学习过程中遇到的棘手问题，让您的 HFSS 学习更加轻松顺畅…

课程网址：http://www.edatop.com/peixun/hfss/11.html

HFSS 天线设计培训课程套装

套装包含 6 门视频课程和 1 本图书，课程从基础讲起，内容由浅入深，理论介绍和实际操作讲解相结合，全面系统的讲解了 HFSS 天线设计的全过程。是国内最全面、最专业的 HFSS 天线设计课程，可以帮助您快速学习掌握如何使用 HFSS 设计天线，让天线设计不再难…

课程网址：http://www.edatop.com/peixun/hfss/122.html

更多 HFSS 视频培训课程：

- **两周学会 HFSS —— 中文视频培训课程**
  课程从零讲起，通过两周的课程学习，可以帮助您快速入门、自学掌握 HFSS，是 HFSS 初学者的最好课程，网址：http://www.edatop.com/peixun/hfss/1.html
- **HFSS 微波器件仿真设计实例 —— 中文视频教程**
  HFSS 进阶培训课程，通过十个 HFSS 仿真设计实例，带您更深入学习 HFSS 的实际应用，掌握 HFSS 高级设置和应用技巧，网址：http://www.edatop.com/peixun/hfss/3.html
- **HFSS 天线设计入门 —— 中文视频教程**
  HFSS 是天线设计的王者，该教程全面解析了天线的基础知识、HFSS 天线设计流程和详细操作设置，让 HFSS 天线设计不再难，网址：http://www.edatop.com/peixun/hfss/4.html
- **更多 HFSS 培训课程**，敬请浏览：http://www.edatop.com/peixun/hfss

关于易迪拓培训：

易迪拓培训(www.edatop.com)由数名来自于研发第一线的资深工程师发起成立，一直致力和专注于微波、射频、天线设计研发人才的培养；后于 2006 年整合合并微波 EDA 网(www.mweda.com)，现已发展成为国内最大的微波射频和天线设计人才培养基地，成功推出多套微波射频以及天线设计相关培训课程和 ADS、HFSS 等专业软件使用培训课程，广受客户好评；并先后与人民邮电出版社、电子工业出版社合作出版了多本专业图书，帮助数万名工程师提升了专业技术能力。客户遍布中兴通讯、研通高频、埃威航电、国人通信等多家国内知名公司，以及台湾工业技术研究院、永业科技、全一电子等多家台湾地区企业。

我们的课程优势：

※ 成立于 2004 年，10 多年丰富的行业经验

※ 一直专注于微波射频和天线设计工程师的培养，更了解该行业对人才的要求

※ 视频课程、既能达到现场培训的效果，又能免除您舟车劳顿的辛苦，学习工作两不误

※ 经验丰富的一线资深工程师讲授，结合实际工程案例，直观、实用、易学

联系我们：

※ 易迪拓培训官网：http://www.edatop.com

※ 微波 EDA 网：http://www.mweda.com

※ 官方淘宝店：http://shop36920890.taobao.com